A study of the paraelectric-ferroelectric phase transition of triglycine sulphate by deuteron nuclear magnetic resonance and relaxation

1989 J. Phys.: Condens. Matter 1 5931

(http://iopscience.iop.org/0953-8984/1/34/011)

J. Phys.: Condens. Matter 1 (1989) 5931–5954. Printed in the UK

A study of the paraelectric–ferroelectric phase transition of triglycine sulphate by deuteron nuclear magnetic resonance and relaxation

Genowefa Ślósarek†, A Heuer‡, H Zimmermann‡ and U Haeberlen‡

† Institute of Bioorganic Chemistry, Polish Academy of Sciences, Noskowskiego 12/14, 61-794 Poznań, Poland

‡ Max-Planck-Institut für Medizinische Forschung, Arbeitsgruppe Molekülkristalle, Jahnstrasse 29, 6900 Heidelberg, Federal Republic of Germany

Received 12 December 1988

Abstract. The quadrupole coupling (QC) tensors of the deuterons in all hydrogen positions are reported for the paraelectric (p) phase of triglycine sulphate (TGS), while for the ferroelectric (f) phase we restrict ourselves to the deuterons in the 'long' and 'short' hydrogen bonds and to the ND_3 deuterons of glycine GI. In addition, the orientation dependence of the spin–lattice relaxation rate $1/T_1$ of the ND_3 deuterons of GI and the temperature dependence of $1/T_1$ of the CD_2 deuterons are reported for the p phase. It is shown that the QC tensors and the relaxation rates of the ND_3 and CD_2 groups of GI can be described well by a dynamic order–disorder model of the phase transition. Any displacive-type model can be ruled out. The temperature dependence of the order parameter p is determined. The CD_2-ND_3 group of GI flips as a rigid unit between the two sides with a correlation time τ_f. The ND_3 group reorients in addition about the C–N bond with a correlation time τ_r. At $T = T_c + 6$ K, $\tau_r = (2.1 \pm 0.2) \times 10^{-11}$ s, $\tau_f = (1.3 \pm 0.2) \times 10^{-11}$ s; τ_f does not vary measurably in the temperature range from T_c to $T_c + 40$ K. At the phase transition there is no critical slowing down of the flip rate. The QC tensors of the CD_2 deuterons are used for a significant refinement of the neutron diffraction structure determination of TGS.

1. Introduction

Matthias *et al* (1956) discovered the ferroelectric properties of triglycine sulphate (TGS). This triggered a long series of investigations of this compound by a wide variety of methods. The dynamics of the various molecular units in TGS was studied, in particular, by proton and nitrogen nuclear magnetic resonance (NMR) and, as well, by deuteron NMR of specifically deuterated crystals of TGS, to be called DTGS (Bjorkstam 1967, Blinc *et al* 1961, 1966, 1967, 1971, Brosovski *et al* 1974, Buchheim and Grande 1975, Buchheim *et al* 1976, Grande *et al* 1978, Hoffmann and Szczepaniak 1979, Lösche 1966, Lösche *et al* 1970, Müller and Petersson 1976, Ślósarek 1983, Ślósarek *et al* 1982, Stankowski 1981, Stepisnik and Slak 1975, Tsujimi *et al* 1978).

From these experiments the general conclusion has been drawn that the crucial molecular units for the phase transition are the NH_3 group of the glycine ion GI on the one hand, and the hydrogen bond between the glycine ions GII and GIII on the other

0953-8984/89/345931 + 24 $02.50

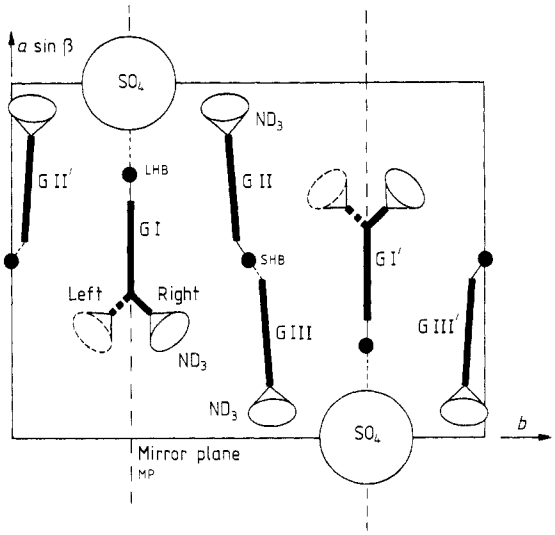

Figure 1. The arrangement of the molecular groups in the unit cell of triglycine sulphate (TGS).

hand (cf figure 1). In labelling the glycine ions we follow the notation of Hoshino *et al* (1959). Judging from the behaviour of the hydrogen bond between GII and GIII, the phase transition appears to be of the order–disorder type. This means that the hydrogen-bonding proton (deuteron) occupies one of two available positions along the hydrogen bond irregularly and with equal probability in the paraelectric phase (p phase), whereas in the ferroelectric phase (f phase) it occupies one of these positions preferentially.

A displacive as well as an order–disorder model has been proposed to describe the dynamics and the role of the NH_3 group of GI during the phase transition. The proponents of the order–disorder model assert that in the p phase this group occupies one of two available positions left and right of the mirror plane designated MP in figure 1. Throughout the crystal the left and right positions are said to be occupied statistically, irregularly and with equal probabilities, i.e. the crystal is disordered. This model is supported most strongly by results of neutron scattering experiments, which indicate that the NH_3 group of GI occupies these two positions (Kay 1977). In figure 2 we show the GI ion in its two configurations. Note that scattering experiments do not allow one to tell whether the disorder is static or dynamic. In either case the plane MP is a mirror plane of the crystal only in a statistical sense. The ^{14}N NMR data show that the disorder is dynamic (Blinc *et al* 1971), i.e. the NH_3 groups are flipping back and forth between their sites left and right of MP. No data about the timescale of this flip process have been obtained so far. As the CO_2 end-group of the GI ion is, according to the neutron data, essentially motionless, the flips of the NH_3 group must be jumps around the central C–C bond of the glycine molecule. As the directions of the bonds of a carbon atom are very rigid, a flip of the NH_3 group results in a concomitant flip of the CH_2 group (see figure 2). In what follows we will, therefore, denote the flips as flips of the CH_2–NH_3 group. The flip process can then be studied by NMR and relaxation of the NH_3 (ND_3) group and, as well, by that of the CH_2 (CD_2) group.

According to the order–disorder model the two available positions of the CH_2–NH_3 group become inequivalent and therefore unequally occupied at the paraelectric–

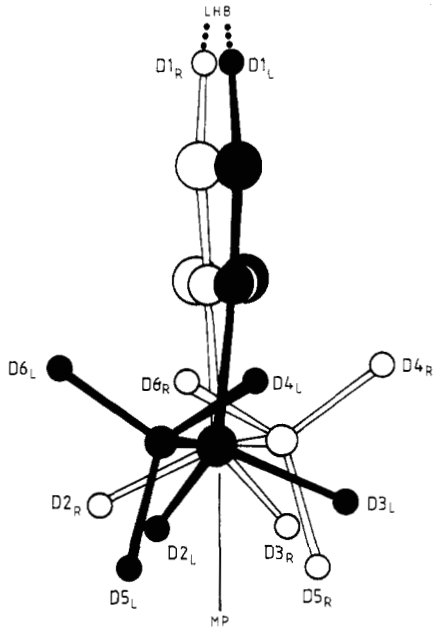

Figure 2. The glycine ion GI with its ND_3 head-group right (R) and left (L) of the plane MP. Note that the CD_2 deuterons jump as well through a large angle whereas the other atoms of the ion remain nearly stationary.

ferroelectric phase transition. The mean electric dipole moment connected with the NH_3 group becomes non-zero at the transition and is considered to be the source of the spontaneous polarisation of the TGS crystal.

According to the other model, the phase transition in TGS is, inasmuch as the CH_2–NH_3 group of GI is concerned, of displacive type. In the p phase the NH_3 group of GI is claimed to occupy, together with the other heavy atoms of this glycine ion, a position right on the plane MP. The only motion of this group is supposed to be a hindered jump–rotation of the NH_3 group about the C–N bond. If this picture is correct, and if we ignore the hydrogens, the plane MP is a genuine mirror plane. When the temperature is lowered below T_c the NH_3 group moves, according to this model, away from the plane MP and results in the appearance of a spontaneous polarisation P_s. This model has emerged from deuteron NMR studies of the ND_3 groups of crystals of DTGS (Blinc *et al* 1967, Bjorkstam 1967, Hoffmann and Szczepaniak 1979).

Proton spectra of the CH_2 group have been observed by Hoffmann and Szczepaniak (1979) and have been interpreted on the basis of the displacive model of the phase transition. No data have been reported so far from deuterated methylene groups, CD_2.

In this paper we present results of deuteron NMR and relaxation measurements of specifically ND_3 and CD_2 deuterated crystals of DTGS. The spectra from the CD_2 group provide additional unequivocal evidence that the phase transition in TGS is of the order–disorder type. We then demonstrate by a realistic calculation of the quadrupole coupling tensor of the ND_3 deuterons that the present and all previous NMR data from this group can readily be interpreted by the order–disorder model, and, in fact, contradict the displacive-type model.

The spin relaxation of the ND_3 group is shown to result from a complicated superposition of contributions from rotational reorientations of the ND_3 group about the C–N

bond and from flips of the whole CH_2–ND_3 group. By contrast the relaxation of the CD_2 deuterons is completely dominated by the flips. The flips can, therefore, be more clearly studied by observing the CD_2 deuterons, while a study of the ND_3 group is necessary to gain information about the rate of the rotational jumps. Indeed, an analysis of the relaxation rates of the ND_3 and CD_2 groups in conjunction with a lineshape analysis of the spectra allows us to derive the rates of the CH_2–ND_3 flips and of the ND_3 rotational jumps in the vicinity of the phase transition.

2. Samples

Triglycine sulphate, $(NH_3^+CH_2COOH)_2(NH_3^+CH_2COO^-)SO_4^{2-}$ (TGS), has been recrystallised three times from D_2O. The product obtained by this procedure possesses deuterated –ND_3 groups and all the hydrogen-bond positions are occupied by deuterons as well. In what follows this material is denoted by DTGS(ND_3).

TGS with deuterated CD_2 groups is denoted by DTGS(CD_2). This material was prepared via perdeuterated glycine obtained by platinum-catalysed exchange with D_2O: Adam's catalyst ($PtO_2 \cdot H_2O$) was pre-reduced by deuterium gas in D_2O, glycine-d_3 (obtained by repeated evaporation of glycine with D_2O) was added, the glass vessel was evacuated and shaken at 150 °C for 5 days. After isolation of the product a second exchange was made under identical conditions. The perdeuterated glycine obtained in this way was back-exchanged in the hydrogen-bond positions with H_2O to obtain glycine-CD_2. The deuteration grade was found by ^1H NMR to be better than 95%. From glycine-CD_2 DTGS(CD_2) was prepared with H_2SO_4 in the conventional manner. Single crystals of DTGS(CD_2) and of DTGS(ND_3) were grown by lowering a saturated H_2O (resp. D_2O) solution of DTGS(CD_2) (resp. DTGS(ND_3)) from 41 °C to room temperature at a rate of 0.1 °C h^{-1}.

From both types of crystals NMR samples were prepared in the form of cylinders about 6–8 mm long and just fitting into 5 mm NMR tubes. In the case of DTGS(ND_3) the (1 0 1), (0 1 0) and ($\bar{1}$ 0 1)* crystallographic axes were chosen as cylinder and, consequently, as rotation axes for recording rotation patterns of line splittings and relaxation rates. For DTGS(CD_2) the (0 1 0), (2 0 $\bar{1}$) and (1 0 2)* axes were chosen as rotation axes.

3. Deuteron quadrupole coupling (QC) tensors

3.1. Experimental results

Deuteron spectra were recorded at $\nu_0 = 54$ MHz either by Fourier-transform NMR or by subjecting the NMR time data to the Cambridge MEM procedure (Sibisi 1983).

Figure 3 presents one of the spectra from the p phase of DTGS(ND_3) obtained by Fourier transformation while figure 4 shows a Cambridge MEM spectrum of DTGS(CD_2). In the figures we have indicated the assignment of the line pairs to the various deuteron sites in these crystals. The assignment is based on a comparison of orientations of the deuteron QC tensors with the deuteron-bond directions, known from structural studies on TGS (Kay 1977, Kay and Kleinberg 1973).

For determining the deuteron QC tensors each sample crystal was rotated in the applied field B_0 in steps of 5° or 10°. From DTGS(ND_3) sets of spectra were recorded at temperatures $T = 281, 303.5, 316, 322.5, 327.5, 331$ and 338 K. The transition from the

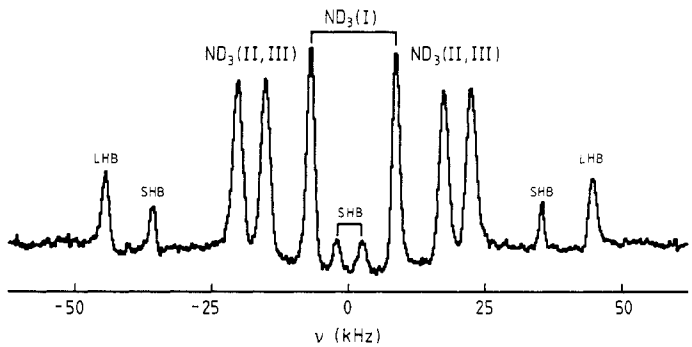

Figure 3. Deuteron Fourier-transform spectrum of DTGS(ND_3). $\boldsymbol{B}_0$ is perpendicular to the (101) axis and subtends an angle of 23.5° with the b axis; T = 338 K; the crystal is in its p phase.

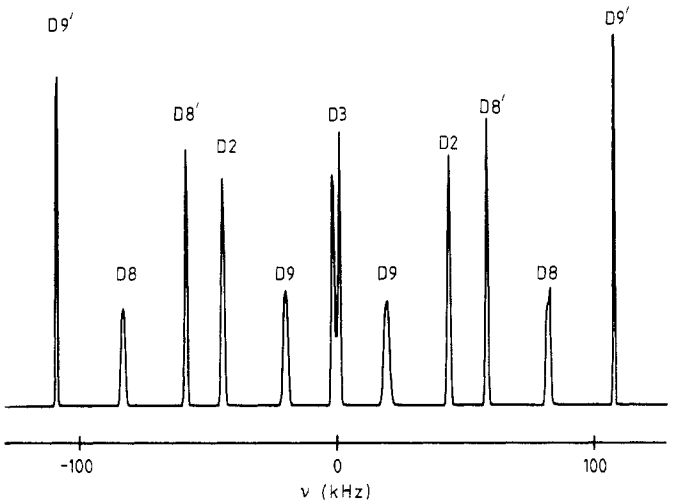

Figure 4. Deuteron Cambridge MEM spectrum of DTGS(CD_2). $\boldsymbol{B}_0 \perp (102)^*$; $\measuredangle(\boldsymbol{B}_0, b) = 28°$; T = 333 K; p phase, D8, D9 arise from the CD_2 groups of the ions GII/III, D8′ and D9′ from those in the mirror reflected positions with respect to MP.

f to the p phase occurred in these crystals at T_c = 331.2 K. For the DTGS(CD_2) crystals a full orientation dependence of deuteron NMR line splittings was only recorded in the p phase at 333 K. For this type of DTGS, T_c = 322 K as in fully protonated crystals. Spectra from the f phase were only recorded for some special crystal orientations (see below). From the measured orientation dependences of the deuteron NMR line splittings the deuteron QC tensors were derived by standard fitting procedures. In table 1 we present the deuteron QC tensors for all deuterons in the p phase of TGS. The assignment of the QC tensors of the CD_2 groups, of which there are no data in the literature, will be explained below. The other deuteron QC tensors from table 1 can be compared with results obtained by Blinc *et al* (1967), Bjorkstam (1967) and Hoffmann and Szczepaniak (1979). As regards the ND_3 groups our results are in essential agreement with previous measurements. On the other hand, our data for the deuterons in the short (SHB) and long (LHB) hydrogen bonds differ from those reported by Blinc *et al* (1967). The discrepancies

Table 1. Deuteron QC tensors of DTGS in p phase. All deuteron QC tensors not specified in the table can be obtained from those listed by applying appropriate symmetry transformations.

Group[b]	Eigenvalue (kHz)	Eigenvector direction[a] θ (deg)	φ (deg)	QCC (kHz)	η
LHB	204.8	99.5	0.2		
$T = 338$ K	−116.3	88.0	89.9	136.5	0.136
D1	−88.5	9.7	−11.9		
SHB	−48.1	85.1	−9.3		
$T = 338$ K	−71.6	106.1	79.3	79.8	0.197
D7	119.6	16.9	97.0		
ND_3	−27.5	69.8	358.1		
GI	−29.4	89.3	88.3	37.9	0.034
$T = 338$ K	56.8	20.2	180.2		
D2	190.7	115.6	117.0		
$T = 333$ K	−122.5	98.4	23.0	127.1	0.285
V_{I}	−68.2	27.2	96.3		
ND_3	78.8	64.5	−3.1		
GII, GIII	−33.3	55.4	106.1	52.6	0.155
$T = 338$ K	−45.5	45.4	238.8		
D8	237.7	122.5	316.2		
$T = 333$ K	−128.3	45.9	264.3	158.4	0.080
V_{II_1}	−109.4	118.4	205.9		
D9	240.1	89.3	68.7		
$T = 333$ K	−128.5	162.3	340.9	160.1	0.070
V_{II_2}	−111.6	107.6	158.4		

[a] In this and in all following tables the spherical coordinates θ and φ are defined with respect to the 'standard orthogonal' (SO) frame with x parallel to the crystallographic axis a, y in the ab-plane and z parallel to c^*, where * refers to the reciprocal frame.

[b] The labelling of the deuterons follows that of table 1 of Kay (1977). D2 belongs to the CD_2 group of GI, D8 and D9 to that of GII, III.

concern the size of the quadrupole coupling constants, the asymmetry parameters and, as well, the temperature dependence of these QC tensors. Therefore, we also report the QC tensors of these deuterons in the f phase of DTGS(ND_3) together with that of the ND_3 group of GI (see table 2).

3.2. Discussion

3.2.1. Deuterons in 'short' (SHB) and 'long' (LHB) hydrogen bonds. The quadrupole coupling constants (QCC) of the deuterons in the SHB (79.8 kHz at $T = 338$ K) and LHB (136.5 kHz) are both exceptionally small on the scale of the QCC of deuterons in other O–D$\cdots$O hydrogen bonds (Berglund *et al* 1978). Drawing on the existing correlation between the O–O distance and the deuteron QCC (see figure 3(*a*) of Mayas *et al* 1978), this implies that the SHB and LHB are both short and are hence strong hydrogen bonds. This statement is confirmed by Kay's structure data (Kay 1977, Kay and Kleinberg 1973), which give O–O = 2.49 Å (SHB) and O–O = 2.59 Å (LHB). According to a similar

Table 2. Deuteron QC tensors of DTGS in f phase.

(*a*) ND_3 group of glycine GI.

Temp. (K)	Eigenvalue (kHz)	Eigenvector direction θ (deg)	Eigenvector direction φ (deg)	QCC (kHz)	η
	−25.8	83.9	±22.9		
281.0	−47.0	90 ± 29.0	90 ± +9.5	48.5	0.291
	72.8	29.8	180 ∓ 56.3		
	−26.8	83.9	±24.9		
303.5	−43.4	90 ± 27.1	90 ± 21.7	46.8	0.237
	70.2	28.0	180 ∓ 53.5		
	−26.8	83.4	±27.6		
316.0	−40.5	90 ± 25.4	90 ± 24.4	44.9	0.204
	67.3	26.4	180 ∓ 48.9		
	−27.2	84.2	±31.9		
322.5	−37.9	90 ± 23.7	90 ± 29.4	43.4	0.165
	65.1	24.5	180 ∓ 45.1		
	−26.9	83.4	±37.0		
327.5	−34.9	90 ± 21.7	90 ± 34.4	41.2	0.129
	61.8	22.7	180 ∓ 37.1		
	−30.9	70.3	±39.9		
331.0	−27.0	90 ± 6.6	90 ± 37.5	38.7	0.067
	58.0	20.8	180 ∓ 19.9		

(*b*) 'Short' hydrogen bond (SHB).

Temp. (K)	Eigenvalue (kHz)	Eigenvector direction θ (deg)	Eigenvector direction φ (deg)	QCC (kHz)	η
	−55.0	88.3	±6.4		
281.0	−78.2	90 ∓ 16.3	90 ± 6.9	88.8	0.175
	133.2	16.4	180 ± 90.4		
	−53.3	87.5	±8.6		
303.5	−76.6	90 ∓ 16.3	90 ± 9.4	86.6	0.179
	129.9	16.5	180 ± 90.0		
	−52.0	87.0	±9.2		
316.0	−75.1	90 ∓ 16.3	90 ± 10.1	84.8	0.182
	127.1	16.6	180 ± 89.0		
	−51.2	86.7	±9.2		
322.5	−74.0	90 ∓ 16.2	90 ± 10.2	83.4	0.182
	125.1	16.6	180 ± 88.1		
	−49.9	86.4	±9.7		
327.5	−73.2	90 ∓ 16.2	90 ± 10.8	82.1	0.189
	123.2	16.6	180 ± 87.4		
	−48.0	85.7	±8.6		
331.0	−72.1	90 ∓ 16.4	90 ± 9.8	80.1	0.200
	120.1	17.0	180 ± 84.2		

Table 2 *continued*

(*c*) 'Long' hydrogen bond (LHB).

Temp. (K)	Eigenvalue (kHz)	Eigenvector direction θ (deg)	Eigenvector direction φ (deg)	QCC (kHz)	η
	204.0	100.0	0.6		
281.0	−116.8	93.5	91.2	136.0	0.145
	−87.3	10.6	20.4		
	204.2	100.6	0.6		
303.5	−116.9	94.2	91.4	136.1	0.145
	−87.3	11.5	22.5		
	204.3	100.6	0.7		
316.0	−116.6	92.3	91.1	136.2	0.141
	−87.7	10.8	13.0		
	204.5	100.7	0.6		
322.5	−116.7	93.2	91.2	136.3	0.141
	−87.9	11.1	17.9		
	204.8	100.6	0.5		
327.5	−116.4	92.8	91.1	136.5	0.137
	−88.3	10.9	15.6		
	204.8	100.4	0.4		
331.0	−116.3	88.3	90.1	136.5	0.136
	−88.5	10.6	−8.9		

empirical but well established correlation between the QCC of the deuteron and the O–D stretching frequency ν_D (Berglund *et al* 1978) we may infer from our results that ν_D is exceptionally small for the SHB, which renders the position of this deuteron a candidate for a crystal instability. The fact that the QCC of the deuteron in the SHB decreases smoothly as T approaches T_c from below, whereas that of the deuteron in the LHB remains independent of T, is direct evidence that the latter has nothing to do with the phase transition while the former plays a key role.

3.2.2. ND_3 groups. The size of the QCC of a stationary N-bonded deuteron is about 150 kHz (Hunt and MacKay 1974). The measured QCC of the ND_3 deuterons of GII/III in the p phase of DTGS(ND_3) is 52.6 kHz and thus roughly a third of the value of a stationary deuteron. This is immediate proof that the group is reorienting rapidly about the C–N axis and that the bond angles of the N atom are approximately tetrahedral.

The QCC of the ND_3 group of GI is substantially smaller (37.9 kHz). This in itself is a strong argument that the dynamics of this group, which is really that of the CH_2–ND_3 group, is more complicated than that of the ND_3 groups of GII/III as is implied by the dynamic order–disorder model of the phase transition. In what follows we focus attention on the dynamics of this group.

Let us denote the probability of occupation of each of the two positions of the ND_3 group as p_L (left) and p_R (right), respectively, with $p_L + p_R = 1$. In the f phase $p_L \neq p_R$, while in the p phase $p_L = p_R = 0.5$. In the f phase p_L and p_R change with temperature.

The average dipole moment connected with the ND_3 group of GI equals

$$\boldsymbol{\mu} = \boldsymbol{\mu}_L p_L + \boldsymbol{\mu}_R p_R \tag{1}$$

where $\boldsymbol{\mu}_L$ and $\boldsymbol{\mu}_R$ are the dipole moments of this group in its left and right positions. The spontaneous polarisation

$$\boldsymbol{P}_s \equiv 2\boldsymbol{\mu}/V \tag{2}$$

is given by

$$\boldsymbol{P}_s = 2(p_R - p_L)\boldsymbol{\mu}_0/V = 2(2p_R - 1)\boldsymbol{\mu}_0/V = 2p\boldsymbol{\mu}_0/V \tag{3}$$

where $\boldsymbol{\mu}_0 = \boldsymbol{\mu}_R = -\boldsymbol{\mu}_L$ and V is the volume of the unit cell. The quantity $p \equiv (2p_R - 1)$ plays the role of the order parameter.

The average QC tensor of the ND_3 group is given by

$$V_{av} = V_L p_L + V_R p_R = \tfrac{1}{2}[(V_R + V_L) + p(V_R - V_L)] \tag{4}$$

with V_L and V_R being the QC tensors of the ND_3 group occupying the left and right positions, respectively.

In the p phase, where $p = 0$, all ND_3 groups of the macroscopic crystal possess the same QC tensor V_{av}. The experimental spectra show only one pair of lines from these groups. This is accounted for if we assume that the group rapidly reorients about the C_N–N bond and that the flip rate is fast on the scale of the quadrupole splittings, which is of the order of 50 kHz. In the f phase, when there is a domain structure in the macroscopic crystal, two pairs of lines will be observed, because there are regions with $p > 0$ ($p_R > p_L$) and others with $p < 0$ ($p_R < p_L$).

Below we calculate V_{av} for the ND_3 group of GI as a function of p. This requires a knowledge of V_L and V_R, which is not available directly from experiment. We calculate V_R on the basis of the following two assumptions:

(i) At each of the three rotational positions of the ND_3 group the instantaneous QC tensor of a deuterium nucleus is axially symmetric about the N–D bond.

(ii) The QCC is given by the empirical formula of Hunt and MacKay (1974):

$$\text{QCC(kHz)} = 253 - 572/R^3 \tag{5}$$

where R is the distance (Å) between the oxygen and the deuterium atom in the N–D$\cdots$O bond. For each of the deuteron positions D4–D6 the distance R and the direction of the N–D bond are derived from the neutron structure data of TGS in the f phase (Kay and Kleinberg 1973). The labelling of the deuterons follows that of Kay and Kleinberg (1973). The structure of DTGS in the paraelectric phase is essentially the same inasmuch as the ND_3 group of GI is concerned (Kay 1977). Using equation (5) the following QCC are obtained:

N–D4:	$R = 1.84$ Å	QCC(4) = 161.2 kHz
N–D5:	$R = 1.72$ Å	QCC(5) = 140.6 kHz
N–D6:	$R = 1.96$ Å	QCC(6) = 177.0 kHz.

Table 3. QC tensors of the ND_3 group of glycine GI for $p = 0$ and $p = 1$ calculated on the basis of the structure of TGS.

p	Eigenvalue (kHz)	Eigenvector direction θ (deg)	Eigenvector direction φ (deg)	η
	−23.1	70.8	0.0	
0	−30.2	90.0	90.0	0.134
	53.2	19.2	180.0	
	−21.3	78.6	347.5	
1	−51.7	63.8	83.2	0.416
	73.0	28.9	236.1	

The components $V_{\alpha\beta}^{(k)}$, $k = 4, 5, 6$, of the QC tensor of each of the deuterons D4, D5 and D6 are given by:

$$\begin{aligned}
V_{xx}^{(k)} &= \tfrac{1}{2}\mathrm{QCC}(k)[3\sin^2\theta(k)\cos^2\varphi(k) - 1] \\
V_{yy}^{(k)} &= \tfrac{1}{2}\mathrm{QCC}(k)[3\sin^2\theta(k)\sin^2\varphi(k) - 1] \\
V_{zz}^{(k)} &= \tfrac{1}{2}\mathrm{QCC}(k)[3\cos^2\theta(k) - 1] \\
V_{zx}^{(k)} &= \tfrac{1}{2}\mathrm{QCC}(k)\sin\theta(k)\cos\theta(k)\cos\varphi(k) \\
V_{zy}^{(k)} &= \tfrac{1}{2}\mathrm{QCC}(k)\sin\theta(k)\cos\theta(k)\sin\varphi(k) \\
V_{xy}^{(k)} &= \tfrac{1}{2}\mathrm{QCC}(k)\sin^2\theta(k)\sin\varphi(k)\cos\varphi(k)
\end{aligned} \tag{6}$$

where $\theta(k)$ and $\varphi(k)$ are the polar angles of the direction of the N–Dk bond in the x, y, z reference frame. Because of the assumed rapid rotational jumps of the ND_3 group the QC tensor V_R is the average of the QC tensors given by equation (6). V_L was calculated analogously.

Knowledge of V_R and V_L enables us now to calculate V_{av} as a function of p (see equation (4)). The results for the two extreme cases $p = 0$ and $p = 1$ are presented in table 3. The first one corresponds to the p phase. So let us compare the calculated $V_{av}(p = 0)$ tensor with the QC tensor of the ND_3 group of GI obtained at $T = 338$ K, $V_{ND_3}(T = 338\ \mathrm{K})$ (see table 1). The eigenvalues of $V_{av}(p = 0)$ are indeed close to the corresponding ones of $V_{ND_3}(T = 338\ \mathrm{K})$, the mean deviation being 2.9 kHz. The principal directions are in good agreement as well, the mean deviation being 0.9°. Apparently there is a difference between the asymmetry parameters but both may be considered as 'small' and so far there is agreement.

V_{av} for $p = 1$ corresponds to the f phase far from the phase transition. $V_{av}(p = 1)$ is to be compared with the experimental data obtained at $T = 281\ \mathrm{K} = T_c - 50\ \mathrm{K}$, $V_{ND_3}(T = 281\ \mathrm{K})$ (see table 2). Apart from the asymmetry parameters $\eta_{calc} = 0.416$ and $\eta_{exp} = 0.291$, the agreement between calculated and measured QC tensors is again satisfactory. For a rapidly reorienting *symmetric* ND_3 group we expect $\eta = 0$. Both the calculation and the experiment give 'intermediate' values of η, indicating clearly a significant deviation of the ND_3 group from C_3 symmetry. As the bond angle and bond length (size-of-QCC) effects on η are intricately interwoven, we dispensed with trying to improve the agreement between calculated and experimental asymmetry parameters by adjusting the bond angles and lengths.

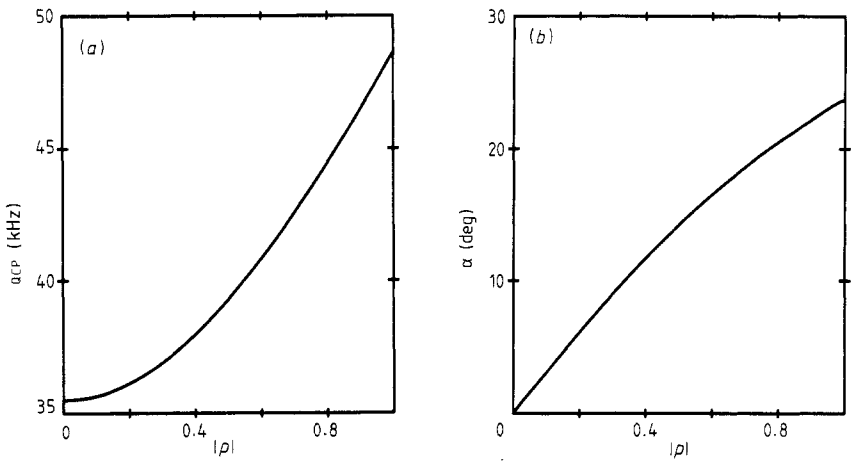

Figure 5. Calculated relations between the order parameter p and (a) the QCC of the ND_3 group of GI and (b) the angle α defined in the text.

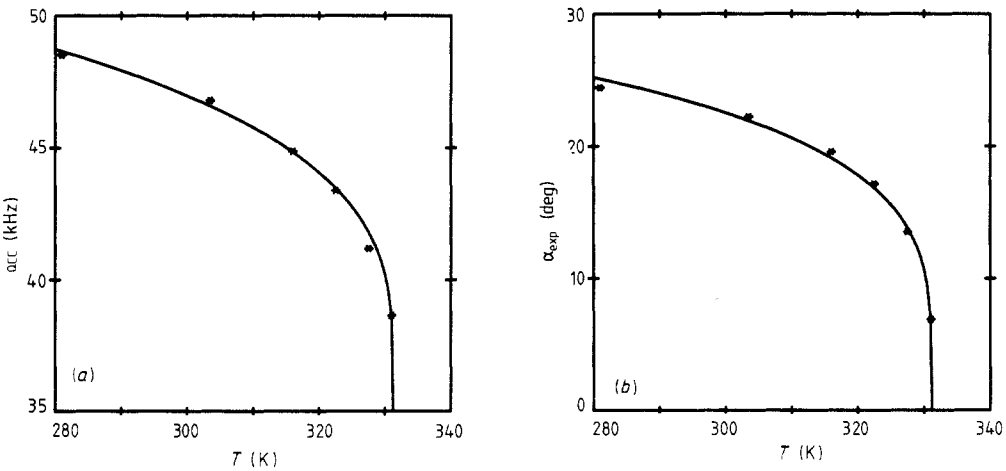

Figure 6. The temperature dependence of (a) the QCC of the ND_3 group of GI and (b) the angle α_{exp}.

The general good agreement between the calculated and experimental QC tensors in the *limiting* cases encourages us to interpret the experimental results in the *intermediate* temperature range with the help of equation (4).

In figure 5 we present the predicted variation with p of the QCC and of the angle $\alpha = [\boldsymbol{e}_z(p), \boldsymbol{e}_z(p = 0)]$; $\boldsymbol{e}_z$ denotes the unique principal direction of $V_{av}(p)$, which is the one associated with the largest principal component. The QCCs and the directions of the z-principal axes of the *measured* QC tensors of the ND_3 group of GI are given in table 2. An experimental angle α_{exp} may be defined in analogy to α. By comparing the values of the QCC and of α_{exp} *measured* as a function of the temperature (see figure 6) with the corresponding *calculated* quantities as a function of the order parameter p, we are able to determine the temperature dependence of this quantity. The results of this comparison

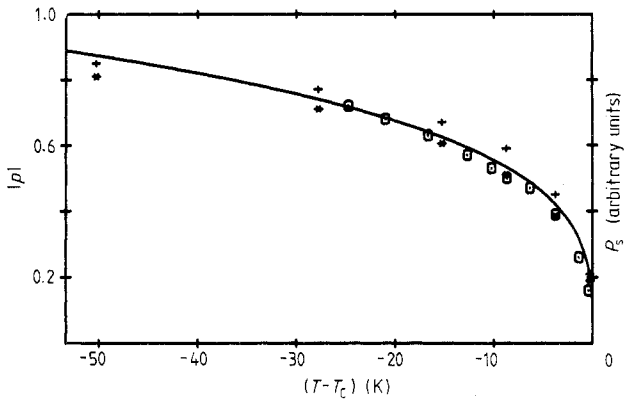

Figure 7. The temperature dependence of the spontaneous polarisation P_s (○) and order parameter p (+, *) in DTGS(ND_3). The values of p are derived from a comparison of calculated (+) and experimental (*) values of QCC and α, respectively.

are shown in figure 7 in which we have also plotted the spontaneous polarisation P_s measured in a DTGS(ND_3) crystal by Stankowska (1985). Generally the character of the temperature dependence of all the plotted quantities is the same. The full curve in figure 7 is a plot of $f(T) = B[(T_c - T)/T_c]^{\beta}$, with $B = 1.49$ and $\beta = 0.28$. According to the Landau theory the critical exponent β is 0.5 if the phase transition is of second order, as it is in the case of fully protonated TGS. The smaller value of β obtained here may be due either to the fact that a rather large range ΔT of temperatures has been included into the fit of the data in figure 7 and/or to the fact that the phase transition in DTGS is intermediate between first and second order. One should notice here that in triglycine selenate, which is isomorphic to triglycine sulphate, deuteration of the crystal causes a change of the order of the phase transition from second to first.

Above we have shown that the QC tensor of the ND_3 group of GI in both the p and f phases of DTGS(ND_3) is described well by the order–disorder model. However, essentially the same deuteron NMR data have been interpreted before according to the displacive model (Blinc *et al* 1967, Bjorkstam 1967, Hoffmann and Szczepaniak 1979). The following arguments were brought forward against the order–disorder model:

(i) The experimental value of η of the QC tensor of the ND_3 group of GI in the p phase is much smaller than expected for the order–disorder model (Blinc *et al* 1967).

(ii) The temperature dependence of the orientation of the unique principal direction of the QC tensor of the ND_3 group could well be interpreted in terms of the displacive model by assuming that this direction is parallel to the direction of the C–N bond of glycine GI (Hoffmann and Szczepaniak 1979).

(iii) In the experimental spectra there is no evidence of broadening of the resonance lines of the ND_3 group of GI near T_c, which is considered to be in contradiction with the order–disorder model (Bjorkstam 1967).

The first of these arguments is based on the assumption that the ND_3 group rotates around a three-fold symmetry axis. As we have discussed above, this assumption is not valid. Only when the realistically calculated QC tensor of the ND_3 group is *averaged over the flip motion* does the asymmetry parameter assume a small value (see table 3).

We reject argument (ii) mainly because it contradicts the neutron diffraction data (Kay 1977). The temperature dependence of the unique principal direction of the QC

tensor of the ND_3 group can be well explained by the order–disorder model. All that is needed is to accept the idea that the flip rate is fast both above and below T_c, i.e. that *there is no critical slowing down of the flip rate at* T_c.

This brings us to argument (iii). The lack of line broadening can be explained naturally if one assumes that the flip rate is fast on the scale of the quadrupole splittings at *all temperatures where the order parameter p differs significantly from unity*. This assumption means that the flip rate is fast in the p phase and, again, that there is no critical slowing down of this rate. In § 4 we demonstrate that the flip rate in the p phase is indeed *very* fast.

3.2.3. CD_2 groups of glycine GI and GII. The spectra of DTGS(CD_2) in the p phase consist of six pairs of lines. Two pairs arise from the CD_2 group of GII and two from GII'. GIII and GIII' are magnetically equivalent to GII and GII', respectively, and so contribute to the same lines. Because GII and GII' are related by the plane MP, the four QC tensors that result from the four line pairs can be grouped into two pairs, which are symmetry-related. As GI and GI' are magnetically equivalent, too, they only give rise to two line pairs. Again, the two resulting tensors must be symmetry-related. Altogether we therefore obtain three independent QC tensors, which we called V_I, V_{II_2} and V_{II_3} in table 1, anticipating their assignment.

V_{II_2} and V_{II_3} are nearly axially symmetric, $\eta_{II_2} = 0.080$, $\eta_{II_3} = 0.070$. Comparison of the unique principal axes of V_{II_1} and V_{II_2} with the neutron data of Kay (1977) reveals that these axes are parallel to the C–D8 and C–D9 bond directions of GII within 2°, so that V_{II_1} and V_{II_2} can be assigned to these deuterons of GII.

The large value of $\eta_I = 0.285$ is immediate evidence that V_I represents an averaged tensor. The unique principal axis of V_I is nearly symmetric to the C–$D2_L$ and C–$D2_R$ bond directions of GI as determined by Kay (1977). It follows that the CD_2 group in GI, actually the CD_2–NH_3 group, undergoes a flip motion between the two directions. This observation confirms the validity of the order–disorder model of the phase transition and completely rules out any displacive model.

In the next step we determine the QC tensors V_{IL} and V_{IR}, which belong to deuteron D2 in the left ($D2_L$) and in the right ($D2_R$) position, respectively. These tensors are needed to analyse the spin–lattice relaxation data to be presented in § 4 and their knowledge enables us to derive C–D2 and C–D3 bond directions, which are more trustworthy than those derived from the neutron scattering data of Kay (1977). Because of the plane MP, deuteron D3 behaves in a symmetrical way and need not be considered separately.

As in the p phase the L and R positions are occupied equally, we get, according to equation (4),

$$V_I = \tfrac{1}{2}(V_{IL} + V_{IR}). \tag{7}$$

A total of 10 independent components are needed to describe V_{IL} and V_{IR}. Five independent equations for them are given by equation (7). To determine V_{IL} and V_{IR} fully we need additional information. As such we could take the C_N–$D2_L$ and C_N–$D2_R$ bond directions derived from the neutron scattering data. These are listed in table 4. The unique principal axis of V_I is symmetric to those bond directions only within 7°. Therefore we do not use the neutron data as additional information.

Instead we assume that for glycine the QC tensor of a carbon-bonded deuteron is a transferable property from site to site. The similarity of the sets of eigenvalues of the QC tensors of D8 and D9 of GII immediately supports this assumption. Therefore it is

Table 4. C–D bond directions in the p phase of TGS according to the neutron data of Kay (1977). His data for D2 yield C–$D2_R$; C–$D2_L$ is obtained by a reflection of C–$D3_R$ with regard to the plane MP.

Glycine	Bond	θ (deg)	φ (deg)
GI	C–$D2_L$	45.1	309.1
	C–$D2_R$	101.7	113.7
GII	C–D8	124.1	318.8
	C–D9	89.9	69.8

Table 5. QC tensors of deuteron D2 in its left (L) and right (R) positions in the p phase of DTGS(CD_2) determined as described in text.

	Eigenvalue (kHz)	Eigenvector direction θ (deg)	Eigenvector direction φ (deg)	QCC (kHz)	η
	238.9	43.8	306.3		
V_{IL}	−128.4	85.0	41.6	159.3	0.075
	−110.5	133.5	316.3		
	238.9	95.1	110.7		
V_{IR}	−128.4	59.3	23.7	159.3	0.075
	−110.5	31.2	192.1		

reasonable to assume that the eigenvalues of V_{IL} and V_{IR} are equal to the respective averaged eigenvalues of V_{II_1} and V_{II_2}. This establishes four further independent relations among the components of V_{IL} and V_{IR}. A final relation can be deduced from the observation that the axis of rotation which transfers V_{IL} into V_{IR} must lie on the plane MP for symmetry reasons.

The resultant system of 10 non-linear equations for the components of V_{IL} and V_{IR} can easily be solved numerically. The tensors V_{IL} and V_{IR} obtained in this way are listed in table 5.

From experimental (see e.g. Müller *et al* 1984) as well as theoretical work (e.g. Weeding *et al* 1985), it is known that the bond direction of a carbon-bonded deuteron coincides to within less than 1° with the unique principal direction of the deuteron QC tensor. We therefore equate the unique principal axes of V_{IL} and V_{IR} with the C–$D2_L$ and C–$D2_R$ bond directions. They differ by 7° and 3° from Kay's (1977) neutron diffraction data. As a test for the accuracy of our procedure of deriving C–D bond directions we calculated the bond angles of the C_N carbons of GI and GII, on the one hand on the sole basis of the neutron data, and on the other hand by taking for the C–D bond directions those determined by NMR (see table 6). We recall that the C_N carbon of glycine is sp^3 hybridised, which implies that the bond angles should display tetrahedral symmetry.

For GII the C_N bond angles are indeed very close to the tetrahedral angle of 109.5°. The closest approach to tetrahedral symmetry is obtained if the C–D bond directions derived by deuteron NMR are taken. It is not clear whether this improvement indicates that our NMR data of GII are more precise than the neutron data or if it only means that

Table 6. Bond angles of the C_N carbon in GI and GII in the p phase of TGS. N: calculated from the neutron structure data. NMR: calculated from the NMR data for the C–D and from the neutron data for the C–C and C–N bond directions.

		Bond angle (deg)	
Group	Bond	N	NMR
GI	$D2–C_N–D3$	100.0	108.1
	$D2–C_N–C$	108.0	106.7
	$D2–C_N–N$	114.2	109.2
	$D3–C_N–C$	109.6	107.2
	$D3–C_N–N$	109.6	110.8
	$C–C_N–N$	114.5	114.5
GII	$D8–C_N–D9$	107.3	109.2
	$D8–C_N–C$	111.9	109.7
	$D8–C_N–N$	110.8	110.7
	$D9–C_N–C$	109.8	109.6
	$D9–C_N–N$	106.6	107.8
	$C–C_N–N$	110.2	110.2

the QC and hence electric field gradient (EFG) tensors have a stronger tendency than the carbon bonds to form tetrahedral angles.

The bond angles of C_N of GI derived solely from the neutron data deviate up to 10° from 109.5°. They conform significantly better to tetrahedral symmetry if the NMR data are taken. This is a strong argument for their correctness. It is interesting to note that those bond angles of C_N from GI which involve the $C–C_N$ bond deviate from the tetrahedral angle by up to 5°, even if we take the NMR directions for the C_N–D bonds. This points to an inaccurate C_N position in Kay's (1977) data, which is undoubtedly due to the motion of the whole C_NH_2–NH_3 group. This statement should not be misinterpreted as saying that we question the general validity of Kay's structural work on TGS.

4. Spin–lattice relaxation

4.1. Experimental results

The orientation dependence of the deuteron spin–lattice relaxation rates $1/T_1$ of the various deuterons of DTGS(ND_3) samples was measured at $T = 338$ K, using the sequence

$$(\pi/2)_{\text{eff}}—t—(\pi/2)_{\text{eff}}$$

where $(\pi/2)_{\text{eff}}$ denotes a

$$20°_x—\tau—110°_{-x}$$

composite $\pi/2$ pulse with $\omega_1\tau = 20°$ (Ślósarek and Haeberlen 1986). The free induction decay (FID) following the second $(\pi/2)_{\text{eff}}$ pulse was recorded, Fourier-transformed and the height of both components of each line pair measured. The ND_3 groups of GII/III relax 'fast', $T_1 \simeq 5$ ms, and the deuterons in the hydrogen bonds SHB and LHB relax 'slowly', $T_1 \simeq 30$ s. The actual values depend on the crystal orientation. Here we focus attention on the ND_3 group of GI, which relaxes at an intermediate rate, $T_1 \simeq 150$ ms. For the determination of the orientation dependence of $1/T_1$ of this group we chose only

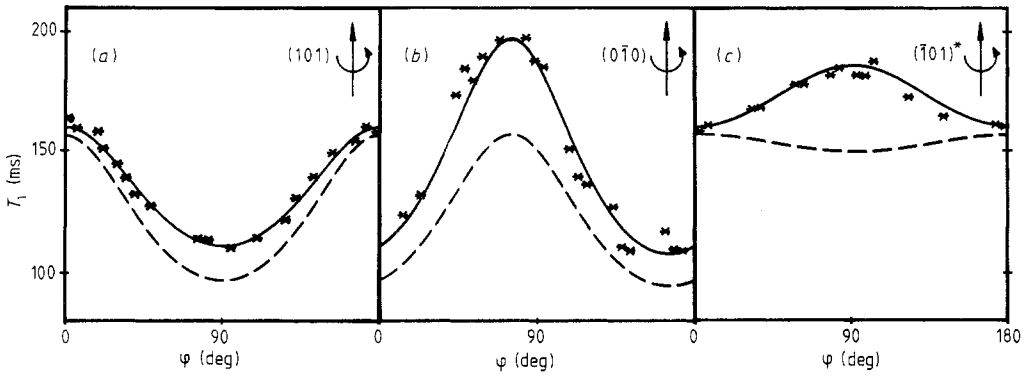

Figure 8. The orientation dependence of the spin–lattice relaxation time T_1 of the ND_3 group of GI in DTGS(ND_3) at $T = 338$ K. (*a*) $\boldsymbol{B}_0 \perp (101)$, $\boldsymbol{B}_0 \| b$ for $\varphi = 0°$; (*b*), $\boldsymbol{B}_0 \perp \boldsymbol{B}_0 \| (\bar{1}01)^*$ for $\varphi = 0°$; (*c*) $\boldsymbol{B}_0 \perp (\bar{1}01)^*$, $\boldsymbol{B}_0 \| b$ for $\varphi = 0°$. Broken curves: expected orientation dependence of T_1 for displacive model. Full curves: best fit to equation (20); see text.

Table 7. Temperature dependence in p phase of relaxation rate $1/T_1$ of deuteron D2 in DTGS(CD_2) for $\boldsymbol{B}_0$ parallel to $(102)^*$.

Temp. (K)	323	335	347	361
$1/T_1$ (s^{-1})	0.48	0.48	0.50	0.47

those crystal orientations where the resonance lines of the $-ND_3$ group of GI were well resolved. The results are shown in figure 8.

In the case of DTGS(CD_2) the temperature dependence of $1/T_1$ was measured from 323 to 360 K for one particular crystal orientation. The results are listed in table 7.

4.2. Discussion

4.2.1. ND_3 group of GI in p phase. The most important feature of the data presented in figure 8 is a pronounced orientation dependence of $1/T_1$. In what follows we shall relate it to the dynamic order–disorder model. To do so we first derive an expression for the relaxation rate of an ND_3 group, which carries out rotational jumps with a correlation time τ_r as well as flips with a correlation time τ_f. Both these motions cause relaxation by modulating the electric field gradient and thus the QC tensor at the site of the deuterons. For each deuteron the instantaneous QC tensor with quadrupole coupling constant QCC is assumed to be axially symmetric about the direction of the N–D bond. For the present purpose it is adequate to assume C_3 symmetry with regard to the rotational jumps. The relaxation rate $1/T_1$ is given by (Spiess 1978)

$$1/T_1 = (2/9)\pi^2[4g_{22}(2\omega) + 4g_{2,-2}(-2\omega) + g_{2,1}(\omega) + g_{2,-1}(-\omega)] \tag{8}$$

where ω is the nuclear Larmor frequency and

$$g_{lm}(n\omega) = \int_0^\infty f_{lm}(\tau) \exp(in\omega\tau)\, d\tau \tag{9}$$

is the spectral density of the correlation function

$$f_{lm}(\tau) = \langle V_{lm}(t) V_{lm}^*(t+\tau) \rangle. \tag{10}$$

The V_{lm} are the spherical components of the *fluctuating* part of the QC tensor. To specify

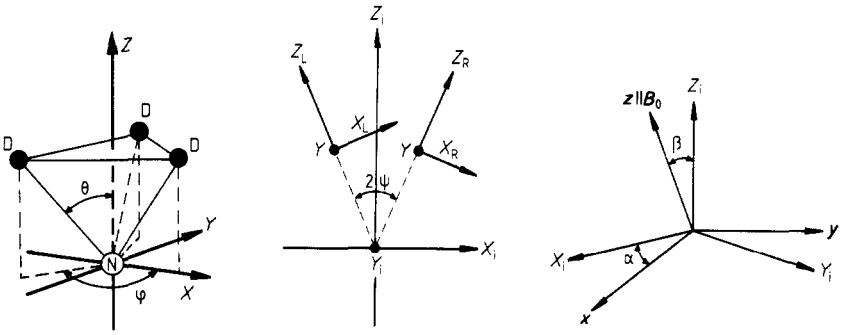

Figure 9. Reference frames introduced for describing a flipping and jump–rotating NH_3 group; see text.

the time dependence of the V_{lm} we define three different reference frames, which are shown in figure 9. The Z axis of the first one (X, Y, Z) is parallel to the assumed C_3 symmetry axis of the ND_3 group. Y lies in the plane MP. We then need an intermediate frame X_i, Y_i, Z_i with X_i normal to the MP plane, $Y_i \| Y$ is normal to the plane spanned by the C_3 symmetry axis in the left (Z_L) and right (Z_R) positions of the flipping ND_3 group, with Z_i bisects Z_L and Z_R. The flip angle is 2ψ. The third is the laboratory frame x, y, z with z parallel to the magnetic field $\boldsymbol{B}_0$. It is related to the X_i, Y_i, Z_i frame by the Euler angles α, β, γ (γ is actually redundant). QC tensor components in these frames are denoted by V^M_{lm}, V^i_{lm} and V_{lm}, respectively. A caret ($\hat{}$) is used to denote tensor components with zero time average.

In the X, Y, Z frame the QC tensor has the following form:

$$\begin{aligned} V^M_{20}(t) &= (3/4)\sqrt{(3/2)}\,\mathrm{QCC}\,3(\cos^2\theta - 1) \\ V^M_{2,\pm1}(t) &= \pm(9/8)\,\mathrm{QCC}\sin 2\theta \exp[.i\varphi(t)] \\ V^M_{2,\pm2}(t) &= \pm(9/8)\,\mathrm{QCC}\sin^2\theta \exp[\mp 2i\varphi(t)]. \end{aligned} \tag{11}$$

Here θ is the angle between the N–D bond and the C_3 axis; $\varphi(t)$ can assume three values: φ_0, $\varphi_\pm = \varphi_0 \pm 120°$. Transforming the V^M_{lm} to the intermediate frame X_i, Y_i, Z_i we obtain

$$\begin{aligned} V^i_{20} &= (3/2)\sqrt{(3/32)}\,\mathrm{QCC}\,\{(3\cos^2\theta - 1)[3\cos^2\psi(t) - 1] \\ &\quad + 3\sin 2\theta \sin 2\psi(t)\cos\varphi(t) \\ &\quad + 3\sin^2\theta \sin^2\psi(t)\cos 2\varphi(t)\} \\ V^i_{2,\pm1} &= \pm(9/16)\,\mathrm{QCC}\,\{\sin 2\psi(t)(3\cos^2\theta - 1) - 4\sin 2\theta\cos^2\psi(t)\cos\varphi(t) \\ &\quad + 2\sin^2\theta \sin\psi(t)[\pm i\sin 2\varphi(t) - \cos\psi(t)\cos 2\varphi(t)] \\ &\quad + 2\sin 2\theta[\cos\varphi(t) \pm i\cos\psi(t)\sin\varphi(t)]\} \\ V^i_{2,\pm2} &= (9/16)\,\mathrm{QCC}\{\sin^2\psi(t)(3\cos^2\theta - 1) \\ &\quad + 2\sin 2\theta \sin\psi(t)[\pm i\sin\varphi(t) - \cos\varphi(t)\cos\psi(t)] \\ &\quad + \sin^2\theta[(1 + \cos^2\psi(t))\cos 2\varphi(t) \mp 2i\cos\psi(t)\sin 2\varphi(t)]\}. \end{aligned} \tag{12}$$

To get the *fluctuating part* of the V^{i}_{lm} we must subtract the time averages

$$\begin{aligned} &\langle V^{i}_{20}\rangle_t = (3/2)\sqrt{(3/32)}\ \mathrm{QCC}(3\cos^2\theta - 1)(3\cos^2\psi - 1) \\ &\langle V^{i}_{2,\pm1}\rangle_t = 0 \qquad \langle V^{i}_{2,\pm2}\rangle_t = (9/16)\ \mathrm{QCC}\sin^2\psi(3\cos^2\theta - 1) \end{aligned} \tag{13}$$

The *time-dependent parts* of the V^{i}_{lm} with *zero time average* are

$$\begin{aligned} \hat{V}^{i}_{20}(t) &= (9/8)\sqrt{(3/2)}\ \mathrm{QCC}\,[\sin 2\theta \sin 2\psi(t)\cos\varphi(t) + \sin^2\psi(t)\sin^2\theta\cos 2\varphi(t)] \\ \hat{V}^{i}_{2,\pm1}(t) &= \pm(9/16)\ \mathrm{QCC}\,\{\sin 2\psi(t)(3\cos^2\theta - 1) - 4\sin 2\theta\cos^2\psi(t)\cos\varphi(t) \\ &\quad + 2\sin^2\theta\sin\psi(t)[\pm \mathrm{i}\sin 2\varphi(t) - \cos\psi(t)\cos 2\varphi(t)] \\ &\quad + 2\sin 2\theta[\cos\varphi(t) \pm \mathrm{i}\cos\psi(t)\sin\varphi(t)]\} \\ \hat{V}^{i}_{2,\pm2}(t) &= (9/16)\ \mathrm{QCC}\{2\sin 2\theta\sin\psi(t)[\pm \mathrm{i}\sin\varphi(t) - \cos\psi(t)\cos\varphi(t)] \\ &\quad + \sin^2\theta[(1+\cos^2\psi(t))\cos 2\varphi(t)) \mp 2\mathrm{i}\cos\psi(t)\sin 2\varphi(t)]\}. \end{aligned} \tag{14}$$

The $\hat{V}^{i}_{2m}(t)$ must now be transformed into the laboratory frame,

$$\hat{V}_{2m}(t) = \sum_{m'} \hat{V}^{i}_{2m'}(t) D^{2}_{m'm}(\alpha, \beta, \gamma) \tag{15}$$

where $D^{2}_{m'm}(\alpha, \beta, \gamma)$ is the Wigner rotation matrix.

The correlation functions (equation (10)) contain terms like $\langle\cos\psi(t)\cos\varphi(t)\cos\psi(t+\tau)\cos\varphi(t+\tau)\rangle$. To evaluate these expressions we assume statistical independence of the jump–rotation and flip motions, which means

$$\begin{aligned} &\langle\cos\psi(t)\cos\varphi(t)\cos\psi(t+\tau)\cos\varphi(t+\tau)\rangle \\ &\quad = \langle\cos\psi(t)\cos\psi(t+\tau)\rangle\langle\cos\varphi(t)\cos\varphi(t+\tau)\rangle. \end{aligned} \tag{16}$$

The factored correlation functions (equation (16)) are calculated according to the general prescription

$$\langle f(t)f(t+\tau)\rangle = \sum_{i=1}^{n}\sum_{j=1}^{n} p_i f_i P(i, t|j, t+\tau) f_j \tag{17}$$

where all symbols have their standard meaning. The conditional probabilities $P(i, t|j, t+\tau)$ are derived from the Kolmogorov equation (Toda *et al* 1983). For the jump–rotation motion there are three equivalent sites (i.e. $n = 3$):

$$\begin{aligned} &p_i = \tfrac{1}{3} \qquad i = 1, 2, 3 \\ &P(i, t|j, t+\tau) = \begin{cases} \tfrac{1}{3} + \tfrac{2}{3}\exp(-\tau/\tau_r) & \text{for } i = j \\ \tfrac{1}{3} - \tfrac{1}{3}\exp(-\tau/\tau_r) & \text{for } i \neq j. \end{cases} \end{aligned} \tag{18}$$

Here τ_r is the correlation time of the jump–rotation process. The corresponding rate is $\Omega_r = 1/n\tau_r = 1/3\tau_r$. For the flip motion ($n = 2$):

$$p_i = \tfrac{1}{2} \qquad i = 1, 2$$

$$P(i, t|j, t+\tau) = \begin{cases} \tfrac{1}{2} + \tfrac{1}{2}\exp(-\tau/\tau_f) & \text{for } i = j \\ \tfrac{1}{2} - \tfrac{1}{2}\exp(-\tau/\tau_f) & \text{for } i \neq j. \end{cases} \tag{19}$$

Here τ_f is the correlation time of the flips; the flip rate equals $\Omega_f = 1/2\,\tau_f$.

Using these relations we get, for example,

$$\langle \cos\varphi(t) \cos\varphi(t+\tau)\rangle = \tfrac{1}{2}\exp(-\tau/\tau_r).$$

In going through the algebra terms like $\langle \cos\varphi(t) \cos 2\varphi(t+\tau)\rangle$ are also encountered. In general they are non-zero and depend, unlike $\langle \cos\varphi(t) \cos\varphi(t+\tau)\rangle$, on the initial angle φ_0; they are, in fact, proportional to $\cos 3\varphi_0$. They vanish for $\varphi_0 = \pm 30°, \pm 90°$. Note that these are the only angles φ_0 for which a flip leads to a mirror reflected orientation of the ND_3 group with respect to the Y_iZ_i-plane which in TGS is the mirror plane MP. According to the structural data of DTGS $\varphi_0 = 84°$. This is close enough to 90° to justify dropping the terms depending on φ_0. Collecting the remaining ones we finally get

$$\begin{aligned} \frac{1}{T_1} = \frac{9}{64}\pi^2 (\mathrm{QCC})^2 \Bigg\{ & (3\cos^2\theta - 1)\sin^2\psi \left(A_1 \frac{\tau_f}{1+4\omega^2\tau_f^2} + A_2 \frac{\tau_f}{1+\omega^2\tau_f^2} \right) \\ & + \sin^2 2\theta \left[\sin^2\psi \left(A_3 \frac{\tau_c}{1+4\omega^2\tau_c^2} + A_4 \frac{\tau_c}{1+\omega^2\tau_c^2} \right) \right. \\ & \left. + A_5 \frac{\tau_r}{1+4\omega^2\tau_r^2} + A_6 \frac{\tau_r}{1+\omega^2\tau_r^2} \right] \\ & + \sin^4\theta \left[\sin^2\psi \left(A_7 \frac{\tau_r}{1+4\omega^2\tau_r^2} + A_8 \frac{\tau_r}{1+\omega^2\tau_r^2} \right. \right. \\ & \left. + A_9 \frac{\tau_c}{1+4\omega^2\tau_c^2} + A_{10} \frac{\tau_c}{1+\omega^2\tau_c^2} \right) \\ & \left. + A_{11} \frac{\tau_r}{1+4\omega^2\tau_r^2} + A_{12} \frac{\tau_r}{1+\omega^2\tau_r^2} \right] \Bigg\} \end{aligned} \tag{20}$$

where τ_c is defined by

$$1/\tau_c = 1/\tau_r + 1/\tau_f.$$

The coefficients A_1 to A_{12} are functions of the Euler angles α and β and describe the orientational dependence of T_1:

$$A_1 = \sin^2 2\beta \cos^2\alpha + 4\sin^2\beta \sin^2\alpha$$

$$A_2 = \cos^2 2\beta \cos^2\alpha + \cos^2\beta \sin^2\alpha$$

$$A_3 = 6\cos^2\psi[3\sin^4\beta - 2\cos 2\alpha(1-\cos^4\beta)] + 2(1+\cos^2\beta)^2 \times (1-\cos^2 2\alpha \sin^2\psi) + 8\cos^2\beta(1-\sin^2 2\alpha\sin^2\psi)$$

$$A_4 = 6\cos^2\psi \sin^2\beta\cos^2\beta(3+2\cos 2\alpha) + 2\sin^2\beta[\cos^2\beta(1-\cos^2 2\alpha\sin^2\psi) + (1-\sin^2 2\alpha\sin^2\psi)]$$

$$A_5 = 8\sin^2\beta[\cos^2\beta(\sin^2\alpha\cos^2\psi + \cos^2\alpha\cos^2 2\psi) + (\cos^2\alpha\cos^2\psi + \sin^2\alpha\cos^2 2\psi)]$$

$$A_6 = 2\cos^2 2\beta(\sin^2\alpha\cos^2\psi + \cos^2\alpha\cos^2 2\psi) + 2\cos^2\beta(\cos^2\alpha\cos^2\psi + \sin^2\alpha\cos^2 2\psi)$$

$$A_7 = 3[\tfrac{3}{2}\sin^4\beta\sin^2\psi + \cos 2\alpha(1-\cos^4\beta)(1+\cos^2\psi)]$$

$$A_8 = 3\sin^2\beta\cos^2\beta[\tfrac{3}{2}\sin^2\psi - \cos 2\alpha(1+\cos^2\psi)]$$

$$A_9 = 2\sin^2 2\beta(1-\cos^2\alpha\sin^2\psi) + 8\sin^2\beta(1-\sin^2\alpha\sin^2\psi)$$

$$A_{10} = 2\cos^2 2\beta(1-\cos^2\alpha\sin^2\psi) + 2\cos^2\beta(1-\sin^2\alpha\sin^2\psi)$$

$$A_{11} = \tfrac{1}{2}(1+\cos^2\beta)^2[\cos^2 2\alpha(1+\cos^2\psi)^2 + 4\sin^2 2\alpha\cos^2\psi] + 2\cos^2\beta[\sin^2 2\alpha(1+\cos^2\psi)^2 + 4\cos^2 2\alpha\cos^2\psi]$$

$$A_{12} = \tfrac{1}{2}\sin^2\beta\{\cos^2\beta[\cos^2 2\alpha(1+\cos^2\psi)^2 + 4\sin^2 2\alpha\cos^2\psi] + [\sin^2 2\alpha(1+\cos^2\psi)^2 + 4\cos^2 2\alpha\cos^2\psi]\}.$$

For equation (20) two limiting cases can be distinguished. The first one, $\psi = 0°$, corresponds to a simple jump–rotational motion of the ND_3 group around the C_3 symmetry axis. It applies to the ND_3 groups of GII/III and within the displacive model of the phase transition in DTGS to the ND_3 group of GI as well. The analogous case of a CD_3 group reorientation has been treated by Tang *et al* (1980). The second limiting case of equation (20), $\psi \neq 0°$, $\theta = 0°$, corresponds to a deuteron jumping back and forth between two positions. It applies to the relaxation of the deuterons of the CD_2 group. From equation (20) we obtain for $\psi = 0°$, $\theta \neq 0°$:

$$\frac{1}{T_1} = \frac{9}{32}\pi^2(\mathrm{QCC})^2\left([\sin^4\theta(1+6\cos^2\beta+\cos^4\beta) + 4\sin^2 2\theta(1-\cos^4\beta)]\frac{\tau_r}{1+4\omega^2\tau_r^2} + [\sin^4\theta(1-\cos^4\beta) + \sin^2 2\theta(4\cos^4\beta - 3\cos^2\beta + 1)]\frac{\tau_r}{1+\omega^2\tau_r^2}\right). \tag{21}$$

This expression agrees with the result obtained by Tang *et al* (1980). For $\psi \neq 0°$, $\theta = 0°$ we get

$$\frac{1}{T_1} = \frac{9}{16}\pi^2(\mathrm{QCC})^2\sin^2 2\psi\left(4\sin^2\beta(\cos^2\beta\cos^2\alpha + \sin^2\alpha)\frac{\tau_f}{1+4\omega^2\tau_f^2} + [\cos^2\alpha(2\cos^2\beta-1)^2 + \cos^2\beta\sin^2\alpha]\frac{\tau_f}{1+\omega^2\tau_f^2}\right). \tag{22}$$

Equation (22) is equivalent to

$$\frac{1}{T_1} = \frac{4}{9}\pi^2\left([(V_{xx}^{fl} - V_{yy}^{fl})^2 + 4(V_{xy}^{fl})^2]\frac{\tau_f}{1+4\omega^2\tau_f^2} + [(V_{xz}^{fl})^2 + (V_{yz}^{fl})^2]\frac{\tau_f}{1+\omega^2\tau_f^2}\right) \tag{23}$$

with $V^{fl} = \frac{1}{2}(V_{IR} - V_{IL})$, which is the expression for $1/T_1$ for a flipping deuteron given by Benz *et al* (1986).

We now try to fit the experimental data from DTGS(ND_3) shown in figure 8 to equation (20). For QCC we take the square root of the average of $(QCC(4))^2$, $(QCC(5))^2$ and $(QCC(6))^2$ calculated for deuterons D4–D6 in § 3. This average is QCC = 160.3 kHz. Likewise we take for θ the average of θ_i of deuterons D4–D6, which is $\theta = 67°$. For ψ we may draw on two sources of information. On the one hand ψ may be identified with α_{exp} for $T \ll T_c$, which is 23.8° (see figure 6). On the other hand we recall that the flips are actually rotations of the CH_2–ND_3 group about the C–C_N bond. As the bonds of the methylene carbon C_N are essentially tetrahedral, the flip angle 2ψ of the C–N bond is equal to that of the C–D_2 bond. The flip angle 2ψ of this latter bond follows immediately from the C–$D2_L$ and C–$D2_R$ bond directions, which were determined in § 3, and turns out to be $2\psi = 44°$. This value compares well with $2\alpha_{exp}$.

This leaves us with τ_r and τ_f to adjust equation (20) to the experimental data. Nevertheless in addition to τ_r and τ_f we let the fitting program search for the optimal values of θ and ψ as well. The best fit was obtained for $\psi = 22.6°$, $\theta = 66.7°$, $\tau_r = 2.2 \times 10^{-11}$ s and $\tau_f = 1.3 \times 10^{-11}$ s ('best-fit parameters'). For $\omega\tau_r \ll 1$ and $\omega\tau_f \ll 1$, as found here, $1/T_1$ depends on QCC only via products $(QCC)^2\tau_r$, $(QCC)^2\tau_f$ and $(QCC)\tau_r\tau_f/(\tau_r + \tau_f)$. Therefore it does not make sense to treat QCC as a separate adjustable parameter. The full curves in figure 8 represent equation (20) with these parameters inserted. The close fit of the full curves to the experimental data demonstrates the validity of the dynamic order–disorder model for TGS. It is reassuring and satisfying that the values obtained for ψ and θ *by the fit of the relaxation data* agree excellently with those determined independently before.

The broken curves in figure 8 represent the orientation dependence of $1/T_1$ for the displacive model, which is described by equation (21). It is obvious that the 'fingerprints' of the models provided by the orientation dependences of $1/T_1$ are sufficiently distinctive to tell the two models apart.

As a matter of fact, an equally good fit of the experimental data to equation (20) as that represented by the 'best-fit parameters' is obtained with the following set of parameters: $\psi = 27.6°$, $\theta = 71.2°$, $\tau_r = 2.0 \times 10^{-11}$ s and $\tau_f = 6.8 \times 10^{-6}$ s. While the values of ψ, θ and τ_r differ somewhat, but not in a substantial manner, from those of the 'best-fit parameters', there is an essential difference regarding the order of magnitude of τ_f. One might be tempted to favour this set of parameters because intuitively we expect that the flips of the bulky CH_2–ND_3 group occur on a much slower timescale than the rotational jumps of the ND_3 group alone. The relaxation data alone are not sufficient to decide whether $\tau_f = 6.8 \times 10^{-6}$ s or $\tau_f = 1.3 \times 10^{-11}$ s. The important decision between these two values is made possible by considering the spectra and relaxation data of the CD_2 group, to which we turn now.

4.2.2. CD_2 group. In figure 10 three deuteron spectra from DTGS(CD_2) are shown. In the spectrum from the p phase (top) we indicate the assignment of the lines from the CD_2 group of GI. In this spectrum we observe from D2 a single line pair arising from an average of V_{IL} and V_{IR} with equal weights p_L and p_R. On cooling the crystal below T_c the line splits into two components corresponding to domains with $p_L - p_R > 0$ and $p_L - p_R < 0$. At $T < T_c - 40$ K a saturation of the line splitting is reached and the two lines correspond to the QC tensors V_{IL} and V_{IR} of deuteron D2 in the L and R positions. The observed frequency difference is $\Delta\nu = 93$ kHz. The width (FWHM) of an NMR line of a deuteron flipping between two sites with equal site occupancies is given in the coalescence regime (Abragam 1961) by

$$\delta\nu = 1/(\pi T_2) + \pi\Delta\nu^2\tau_f \tag{24}$$

where $1/(\pi T_2)$ is the width in the absence of flips. If we equate the measured width

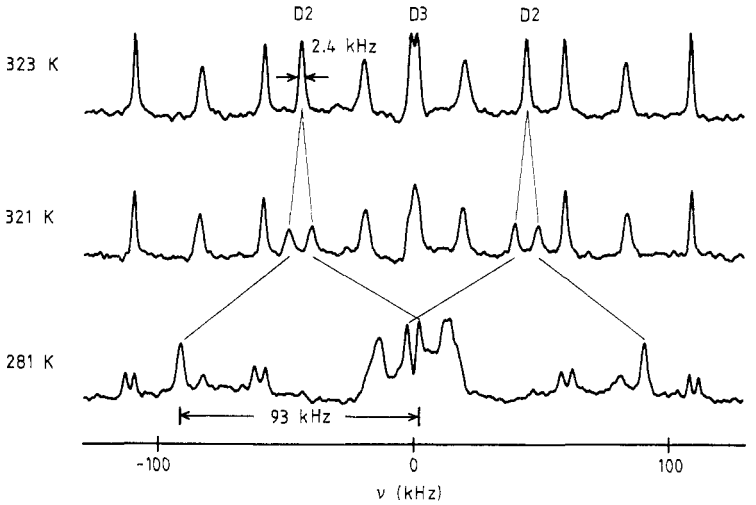

Figure 10. Temperature dependence of deuteron Fourier-transform spectrum of DTGS(CD_2). Same crystal orientation as in figure 3. Note the splitting of the lines from D2 as the temperature is lowered into the f phase. Note also how little the lines split from the methylene groups of GII/III.

$\delta\nu_{exp} = 2.4$ kHz with $\pi\Delta\nu^2\tau_f$ and insert $\Delta\nu = 93$ kHz we get an *upper limit* for τ_f, which is $\tau_f^{(\text{upper limit})} = 9 \times 10^{-8}$ s. This value definitely rules out the set of fit parameters with $\tau_f = 6.8 \times 10^{-6}$ s and we may conclude unequivocally that the correlation time of the flips of the CH_2–ND_3 groups is $\tau_f = 1.3 \times 10^{-11}$ s. The estimated error is 0.2×10^{-11} s.

As mentioned earlier our measurements of $1/T_1$ of the CD_2 group enable us to determine τ_f in an independent manner. The relaxation rate of this group is described by equation (23). As V_{IL} and V_{IR} have been determined before (see table 5) τ_f is the only unknown parameter on the right-hand side of equation (23). According to table 7 $1/T_1 = (0.48 \pm 0.02)\ s^{-1}$ for $T = 323$–361 K. Transforming $V^{fl} = \frac{1}{2}(V_{IL} - V_{IR})$ from the standard orthogonal to the laboratory frame for the particular crystal orientation chosen for the T_1 measurements, inserting the appropriate components of V^{fl} (lab. frame) into equation (23) and solving for τ_f yields $\tau_f = (1.2 \pm 0.2) \times 10^{-11}$ s. This value agrees with the result derived from the ND_3 relaxation data. We note in passing that there is a second solution with $\tau_f = 3.3 \times 10^{-7}$ s, which is ruled again out by $\tau_f^{(\text{upper limit})} = 9 \times 10^{-8}$ s.

The finding that in the p phase of TGS the CH_2–ND_3 group of GI flips by an angle $2\psi \simeq 44°$ with a correlation time as short as 1.2×10^{-11} s is the key experimental result of this work. It implies exceptional freedom of this group to move in the crystal lattice. This statement is strengthened by observing that the correlation time of the *rotational* jumps of the ND_3 part of this group, $\tau_r = 2.1 \times 10^{-11}$ s, is much shorter than the corresponding time for the ND_3 groups of GII/III, which is about 6×10^{-10} s. This value is obtained by inserting the observed relaxation time of this group, $T_1 = 5$ ms, into equation (21), taking the same values for QCC and θ as above and solving for τ_r. The conclusion that the NH_3 groups of GI are more mobile than those of GII/III has also been inferred from proton relaxation measurements (Ślósarek *et al* 1982).

As the relaxation rate of the CD_2 deuterons hardly changes in the temperature range from 323 to 361 K (see table 7) we must conclude that τ_f itself is essentially independent of T in that range, which is a very surprising result.

It has, however, a counterpart in the temperature and frequency dependence of the dielectric relaxation of TGS, which has been measured carefully by Luther (1973). While the macroscopic dielectric relaxation time τ_ε varies significantly with T in the p phase of TGS, Luther finds that the corresponding microscopic quantity $\tau_0 = 1/(2\pi\tilde{f}_0) = \tau_\varepsilon/(\varepsilon_{\text{static}} - \varepsilon_\infty)$, where $\tilde{f}_0$ is the 'characteristic frequency', is independent of T as is τ_f. The value of τ_0 derived by Luther is, however, as short as 7×10^{-14} s and is hardly realistic as a correlation time for a molecular unit of the size of a CH_2–NH_3 group. We recall that dielectric measurements give no clue as to which molecular group is connected with the observed relaxation process. By contrast, our deuteron NMR measurements demonstrate conclusively that it is the CD_2–NH_3 (CH_2–ND_3) group of the ion GI that flips about the C–C bond with a correlation time of $(1.2 \pm 0.2) \times 10^{-11}$ s.

We recall that the determination of the microscopic quantity τ_0 involves a theoretical model that transfers the directly measured macroscopic relaxation τ_ε into a local quantity. Also, it is worth while pointing out that we find essentially the same values of τ_f for the CD_2–NH_3 and CH_2–ND_3 groups despite the fact that the phase transition temperature T_c is different in DTGS(CD_2) and DTGS(ND_3) by as much as 10 K. This may be taken as a hint that the phase transition itself is not triggered by the CH_2–NH_3 groups of GI, but by the dynamics of the proton (deuteron) in the 'short' hydrogen bond.

Acknowledgments

We would like to express our gratitude to Mrs H Kessel for her help in the tedious calculations leading to equation (20). We acknowledge most helpful discussions with N Pislewski and J Stankowski, as well as a tutorial on macroscopic and local dielectric quantities by J Petersson. We thank J Stankowska for the crystals of DTGS(ND_3) and for rendering available her results on the spontaneous polarisation in that crystal. Much of the experimental work was done when G Ś was a guest from the Institute of Molecular Physics of the Polish Academy of Sciences (Poznań, Poland) at the Max-Planck-Institut für Medizinische Forschung in Heidelberg, from which she appreciates hospitality and a stipend.

References

Abragam A 1961 *Principles of Nuclear Magnetism* (Oxford: OUP)
Benz S, Haeberlen U and Tegenfeldt J 1986 *J. Magn. Reson.* **60** 125
Berglund B, Lindgram J and Tegenfeldt J 1978 *J. Mol. Struct.* **43** 179
Bjorkstam J L 1967 *Phys. Rev.* **153** 599
Blinc R, Detoni S and Pintar M 1961 *Phys. Rev.* **124** 1036
Blinc R, Lahajnar G, Pintar M and Zupancic I 1966 *J. Chem. Phys.* **44** 1784
Blinc R, Mali M, Osredkar R, Prelesnik A and Zupancic I 1971 *J. Chem. Phys.* **55** 4843
Blinc R, Pintar M and Zupancic I 1967 *J. Phys. Chem. Solids* **28** 405
Brosovski G, Buchheim W, Müller D and Petersson J 1974 *Phys. Status Solidi* b **62** 93
Buchheim A and Grande S 1975 *Phys. Status Solidi* a **28** K121
Buchheim A, Grande S, Rosenberger H, Schnabel B and Voigtsberger B 1976 *Ann. Phys., Lpz.* **33** 374
Grande S, Schultz J and Lösche A 1978 *J. Mol. Struct.* **47** 1
Hoffmann S K and Szczepaniak L 1979 *J. Magn. Reson.* **36** 359
Hoshino S, Okaya Y and Pepinsky R 1959 *Phys. Rev.* **115** 323
Hunt M J and MacKay A L 1974 *J. Magn. Reson.* **15** 402
Kay M I 1977 *Ferroelectrics* **17** 415
Kay M I and Kleinberg R 1973 *Ferroelectrics* **5** 45

Lösche A 1966 *Rev. Roum. Phys.* **11** 841
Lösche A, Grande S and Windsch W 1970 *Proc. XVI Congr. AMPERE* p 143
Luther G 1973 *Phys. Status Solidi* a **20** 227
Matthias B T, Miller C E and Remeika J P 1956 *Phys. Rev.* **104** 849
Mayas L, Plato M, Winscom C J and Möbius K 1978 *Mol. Phys.* **36** 735
Müller C, Schajor W, Zimmermann H and Haeberlen U 1984 *J. Magn. Reson.* **56** 235
Müller D and Petersson J 1976 *Phys. Status Solidi* b **78** 191
Sibisi S 1983 *Nature* **301** 134
Ślósarek G 1983 *PhD Thesis* Poznań
Ślósarek G and Haeberlen U 1986 *Seventh Specialized Colloque AMPERE (Bucharest) 1985* p 377
Ślósarek G, Idziak S, Pislewski N and Stankowski J 1982 *Phys. Status Solidi* b **110** 233
Spiesss H W 1978 *NMR Basic Principles and Progress* vol 15, ed. E Fluck and R Kosfeld (Berlin: Springer) p 55
Stankowska J 1985 unpublished results
Stankowski J 1981 *Phys. Rep.* **77** 1
Stepisnik J and Slak J 1975 *J. Chem. Phys.* **62** 34
Tang J, Pines A and Emid S 1980 *J. Chem. Phys.* **73** 172
Toda M, Kubo R and Saito N 1983 *Statistical Physics II* (Berlin: Springer)
Tsujimi Y, Kasahara M and Tatsuzaki I 1978 *Phys. Lett.* A **65** 366
Weeding T, Kwiram A L, Rawlings D C and Davidson E R 1985 *J. Chem. Phys.* **82** 3516